Continental Shelf Research 289 (2025) 105464

Contents lists available at ScienceDirect

Continental Shelf Research

journal homepage: www.elsevier.com/locate/csr

Distribution of rare earth elements and their signatures from the Mackenzie River delta to the abyssal Arctic Ocean

Thomas Bossé-Demers [a], Charles Gobeil [b], Bennet Juhls [c], Martine Lizotte [d], Michael Fritz [c], Lisa Bröder [e], Atsushi Matsuoka [f], Santiago Mareque [a], Raoul-Marie Couture [a,*]

[a] *Département de Chimie, Takuvik Joint International Laboratory and Centre D'études Nordiques, Université Laval, 1045 Ave. de La Médecine, Québec, QC, G1V 0A6, Canada*

[b] *INRS-Eau Terre Environnement, 490 Rue de La Couronne, Université Du Québec, QC, G1K 9A9, Canada*

[c] *Permafrost Research Section, Alfred Wegener Institute Helmholtz Centre for Polar and Marine Research, Potsdam, Germany*

[d] *Maurice Lamontagne Institute, Fisheries and Oceans Canada, 850 Rte de La Mer, Mont-Joli, QC, G5H 3Z4, Canada*

[e] *Geological Institute, Swiss Federal Institute of Technology (ETH), Zurich, Switzerland*

[f] *Institute for the Study of Earth, Oceans, and Space, University of New Hampshire, 8 College Rd., Durham, NH, 03824, USA*

A B S T R A C T

The Mackenzie River is North America's largest contributor of freshwater and sediment to the Arctic Ocean. Here, we evaluate the potential of rare earth elements (REE) as tracers of its sediment sources and fate, from the river mouth to the deep Arctic Ocean. We collected sediment cores from 21 sites, from the delta to the marine shelves, slopes and basins and measured the spatial and down-core distribution of total, leached and residual REE concentrations. Our results show that the proportion of leached REE is highest in the delta. This proportion decreases with distance from the river, suggesting mixing with other sediment sources, REE loss to the residual phase, or REE scavenging via adsorption and complexation in coastal waters. Normalized REE concentrations plotted against their atomic number provide regional signatures. The leached REE signatures indicate medium REE enrichment in the Mackenzie Delta, an enrichment that diminishes with distance from the delta. We then used a similarity index (SI) to investigate the divergence amongst REE signatures, with riverine and deep marine basin values as endmembers for the calculation. Our results highlight the influence of the Mackenzie Region sediments on the Beaufort Sea margin. Overall, our findings demonstrate that REE are relevant tracers for identifying sediment sources and that tracking REE distribution from the delta to the deep Arctic Ocean offers additional insights into sediment transport mechanisms.

1. Introduction

Arctic river basins are affected by morphological (Ielpi et al., 2023), hydrological (Stadnyk et al., 2021) and biogeochemical (Oziel et al., 2025) changes in response to global climate change. At the same time, Arctic permafrost coasts, which account for 34 % of the world's coastline (Lantuit et al., 2012), are sensitive to erosion [(Nielsen et al., 2022); (Fritz et al., 2017)], with retreat rates that have more than doubled since the 2000s in some parts of the Arctic coastline [(Zhang et al., 2022); (Irrgang et al., 2022)], contributing to an estimated 8-fold increase in sediment loads over the past decades (Zhang et al., 2022).

Sediments from diverse sources are exported to the Arctic Ocean, and the location of their burial is not fully constrained [(Zhang et al., 2021); (Holmes et al., 2002)], which hampers our understanding of interactions between maritime boundaries [(DeRepentigny et al., 2020); (Bostock et al., 2019)], the impact of global warming on sediment supply [(Zhang et al., 2021); (Schwab et al., 2021)] and on the fluxes of organic carbon derived from thawing permafrost [(Nielsen et al., 2022); (Juhls et al., 2022)], and of the fluxes of nutrients which underpin marine biological productivity [(Oziel et al., 2025); (Zhang et al., 2021); (Larkin et al., 2021)]. In this context, we explore the potential to use rare earth elements (REE) as geochemical tracers of sediment sources from rivers to sea, employing the Mackenzie River as a globally relevant case study.

The Mackenzie River, carrying about 128 million tons of sediment load to its delta and adjacent sea each year, is the largest point source of sediment to the Arctic Ocean. It flows through both continuous and discontinuous permafrost zones, and ultimately drains into the Beaufort Sea where it contributes more than twice as much sediment as all the other rivers draining into the Arctic Ocean combined (Kuzyk et al., 2013; Stein et al., 2004; Holmes et al., 2011; Vonk et al., 2015; Carson et al., 1999). In recent years, riverine freshwater discharge has increased due to climate change (Rood et al., 2017). This increase is associated with an observed 46 % rise in suspended particle discharge between 2005 and 2015 (Doxaran et al., 2015).

* Corresponding author.
E-mail address: raoul.couture@chm.ulaval.ca (R.-M. Couture).

https://doi.org/10.1016/j.csr.2025.105464
Received 6 November 2024; Received in revised form 13 March 2025; Accepted 19 March 2025
Available online 19 March 2025

The application of the relationship between REE concentrations and their atomic numbers, a pattern referred to as a "signature", as a geochemical tracer was first proposed by Piper (1974). A body of literature reports on sedimentary REE signatures and enrichment ratios and uses these to determine the relative contributions of sediment from various end members, with the assumption that REE signatures are source-specific (Lim et al., 2014; Song and Choi, 2009; Xu et al., 2009; Yang et al., 2003). Yet, the use of REE variability to trace sediment sources is not straightforward. Several studies have highlighted that REE in sediments can be divided into distinct leached and residual phases, with the leached phase being more labile and influenced by geochemical processing of the sediment, while the residual phase reflects the source rocks. The leached phase primarily consists of labile REE bound to organic matter, adsorbed onto iron (Fe) and manganese (Mn) oxides and (oxy)hydroxides, carbonates, clays and apatite (Jung et al., 2021), while the residual phase consists largely of recalcitrant compounds such as silicates and aluminosilicates (Su et al., 2017). As such, despite their similarities, REE elements are susceptible to geochemical discrimination based on the nature of the sedimentary matrix (Tadayon et al., 2024a). In this study, we document the spatial distribution and vertical profiles of leached, residual, and total REE concentrations in sediment cores (up to 50 cm deep) from the Mackenzie Delta to the abyssal plains of the Arctic Ocean. We analyze the relative distribution of these phases and construct REE signatures based on normalized concentrations. Finally, we evaluate the relative changes in REE signatures across 21 distinct sites from the Mackenzie River to the central Arctic Ocean, in the context of particulate REE transport and fate.

2. Materials and methods

2.1. Study region

The study area encompasses the Mackenzie Delta and the Arctic Ocean (Figs. 1 and 2) and is divided into six distinct regions. Our study sites cover a range of sediment accumulation rates, with cores representing timescales of a few years in the Mackenzie Region [(Graf Pannatier, 1997); (Goñi et al., 2000)], 100–200 years in the Bering and Chukchi Shelves, Barrow Canyon (Kuzyk et al., 2017), and Beaufort Sea Margin (Kuzyk et al., 2013), and far beyond the Holocene period in the Amerasian Basin (Gobeil et al., 1999).

1) Mackenzie River and Delta (hereafter, "Mackenzie Region"): This region experiences strong seasonal variations, particularly in water discharge (Hill et al., 2001). Conductivity, suspended solids, and dissolved constituents also vary seasonally [(Juhls et al., 2022); (Lizotte et al., 2023); (Emmerton et al., 2008)]. Similarly, salinity ranges from freshwater within the delta to brackish further from the coast [(Juhls et al., 2022); (Lizotte et al., 2023)]. The Mackenzie River is recognized as the major source of sediment to the Arctic Ocean (Vonk et al., 2015), with an average yearly sediment load of 128 Mt. It is itself fed by the Peel (21 Mt), the Arctic Red (7 Mt) and the Liard (35–45 Mt) rivers (Vonk et al., 2015).
2) Bering and Chukchi Shelves: The shallow shelves of these regions are considered among the most biologically productive in the world (Kuzyk et al., 2017). They are greatly influenced by Pacific waters [(Kuzyk et al., 2017); (Grebmeier and Cooper, 1995)] for the Bering Sea, and the Siberian coastal currents and the Atlantic Intermediate Water Mass in the northern part of the Chukchi Sea (Deschamps et al., 2018). The primary sources of sediment to these shelves are from the Yukon River, northeastern Siberia, and the Mackenzie River [(Deschamps et al., 2018); (Darby et al., 2009)].
3) Barrow Canyon: This region is also highly productive, influenced by a range of water masses and sediment sources including the Chukchi Sea [(Lin et al., 2021); (Pickart et al., 2021)] and its slope current (Song et al., 2022), the Beaufort Gyre and Mackenzie River via ice rafted debris [(Deschamps et al., 2018); (Song et al., 2022); (Klotsko et al., 2019)].
4) Beaufort Sea Margin: This region is oligotrophic due to high turbidity from river inputs [(Kuzyk et al., 2017); (Macdonald et al., 1998)]. Its sediment and freshwater input are majorly influenced by the Mackenzie River and its delta [(Vonk et al., 2015); (Kuzyk et al., 2017); (Deschamps et al., 2018); (Klotsko et al., 2019)]. Sea ice transport is an important sediment import process, originating from the Mackenzie River and Delta region, with a smaller proportion from sediment resuspension in the Beaufort Sea [(Eicken et al., 2005); (Hillaire-Marcel et al., 2013)] and the Banks Island area (Darby et al., 2011). These ice rafted debris are a sediment vector

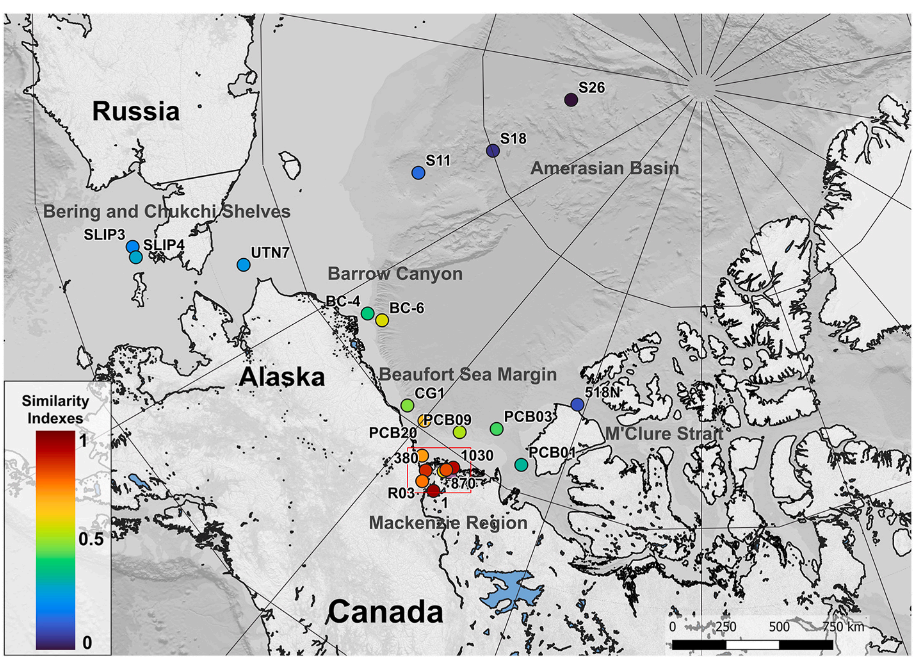

Fig. 1. Location of sampling sites and their similarity index (SI) calculated using stations 1 and S26 as endmembers. The area within the red square is shown in Fig. 2.

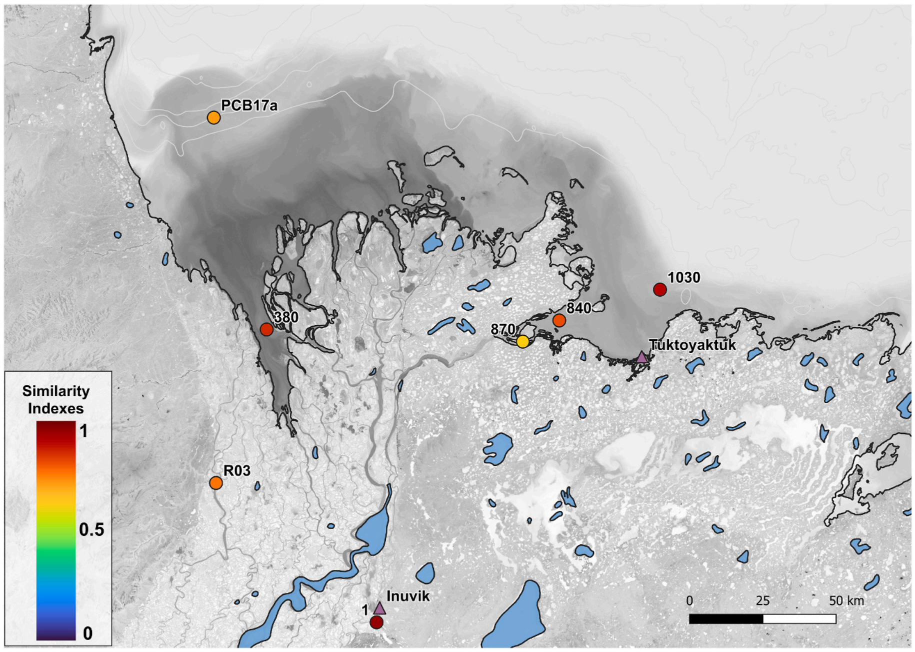

Fig. 2. Location of sampling sites in the Mackenzie River Delta region and their similarity index (SI) calculated using stations 1 and S26 as endmembers (S26 is shown in Fig. 1). Purple triangles indicate settlements in the region where field labs where based.

along the Beaufort Gyre, which is an important clockwise current (Pickart et al., 2021).

5) Amerasian Basin: This region is oligotrophic, with carbon fluxes to the sediment less than 10 g m^2 yr. It is also the deepest area covered in this study [(Gobeil et al., 1999); (Degen et al., 2015)]. This region is mostly influenced by the Transpolar Drift, with direct sediment import from the Laptev Sea and Russians Rivers [(Darby et al., 2011); (Charette et al., 2020)]. Large amounts of sea ice transport occur in the Amerasian Basin, with a high variance in sources due to the transport capacity of ice (Ortiz et al., 2009).
6) M'Clure Strait: Sediment sources at this single station (Station 518N) are solely influenced by the Canadian Arctic Archipelago (Letaïef et al., 2021) and erosion of Banks Island (Agnew et al., 2008), and likely not by the Mackenzie River. Sea ice plays an important role in the delivery of sediment from the surrounding islands (Agnew et al., 2008). This station serves as a control in this study.

2.2. Field work

Field work in the Mackenzie Delta region took place in 2019 (Lizotte et al., 2023). Coastal and fluvial sediment samples were collected from 6 stations (Table 1), either beneath the ice in spring (May), or in open water from boats in late summer (September). The sampling was carried out along a transect from river water within the delta (Station 1; 68.31 °N, 133.67 °W) to coastal waters (Station 1030; 69.64 °N, 133.22 °W). Sediment cores were retrieved at each site using a 9 cm diameter gravity corer (Uwitec, Austria). The sediment cores were relatively short, ranging from 5 to 30 cm in length, due to the sandy and rocky nature of the sediments. No sediment leakages were observed during sampling. As with previous studies at similar sites, compaction was not accounted for [(Kuzyk et al., 2013); (Kuzyk et al., 2017); (Deschamps et al., 2019)-(Kuzyk et al., 2011)]. Cores were subsampled at 1 cm intervals in field labs located in Inuvik or Tuktoyaktuk. Additional details on the sampling campaigns are available in Lizotte et al. (2023) (Lizotte et al., 2023). Beaufort Sea sediments and M'Clure Strait cores (Table 1) were collected aboard the Canadian Coast Guard Ship (CCGS) *Amundsen* in September–October 2021 (Bröder et al., 2022). Cores were collected using a 10 cm diameter multicorer (Oktopus, Germany). At these sites, the core lengths varied between 17 cm and 45 cm. Cores were subsampled directly on the ship at 1 cm intervals.

Table 1
Station locations and water column depths for the sediment cores collected during this study.

Region	Station	Water Depth (m)	Latitude (N)	Longitude (W)
Mackenzie Region	1	1.5	68.318	133.678
	R03	4[a]	68.390	135.429
	840	1[a]	69.398	133.809
	870	4.6	69.282	133.970
	1030	5[a]	69.648	133.221
	380	1.5	68.862	135.833
	PCB17a	20	69.287	137.279
Bering and Chukchi Shelves	SLIP3	73	63.664	174.436
	SLIP4	73	63.676	173.382
	UTN7	58	68.000	168.933
Barrow Canyon	BC4	599	71.880	156.018
	BC6	2125	72.233	154.037
Beaufort Sea Margin	CG1	204	70.562	142.858
	PCB01	411	71.232	125.598
	PCB03	1044	72.113	131.046
	PCB09	675	71.102	135.144
	PCB20	782	70.549	139.819
Amerasian Basin	S11	2265	76.653	173.385
	S18	2860	80.142	173.337
	S26	3130	84.063	175.088
M'Clure Strait	518N	526	74.680	121.450

[a] Estimated under-ice depth.

Sediment cores from the central Arctic basins were sampled in 1994 aboard the CCGS *Louis S. St-Laurent,* while cores from the Bering Sea, the Chukchi Sea, and the Beaufort Sea margin were collected in 2007 aboard the CCGS *Sir Wilfrid Laurier* [(Kuzyk et al., 2017); (Gobeil et al., 1999); (Macdonald and Gobeil, 2011)]. Cores were collected using a box corer and subsampling targeted the middle of the box to avoid smeared or compacted sediment. The cores were subsampled directly on deck, at every 0.5 cm for the top 2 cm, then at 1 cm intervals between 2 and 10 cm, and 2, 3 or 5 cm intervals for the remainder of the core [(Kuzyk et al., 2013); (Kuzyk et al., 2017); (Macdonald and Gobeil, 2011)]. In all cases, subsamples were placed in Whirl-Pak bags (Fisher Scientific, Canada) and stored frozen until they were freeze-dried and homogenized using an agate mortar and pestle.

2.3. Sample treatment

The surface samples for Bering and Chukchi Shelves, Barrow Canyon, Beaufort Sea Margin and Amerasian Basins were digested on a hot plate using HCl, HNO_3 and HF according to Sturgeon et al. (1982) (Sturgeon et al., 1982) and compared to measurements of the LKCD ($n = 14$) sediment certified reference material (CRM) from National Research Council (NRC, Canada). Accuracy was >90 %. The surface sample for the Mackenzie Delta was instead digested using a microwave with HCl and HNO_3 and validated against the MESS-4 CRM (n = 21). Accuracy of the digests against CRMs was <6 %, except for Nd and Yb for which it was <28 %. Total Lu could not be validated.

The leached REE content was assessed by targeted extraction at all stations. 250 mg of dry, homogenized sediment was placed in a 50 mL acid-washed centrifuge tube (VWR, Canada) and amended with 50 mL of 1 N HCl (VWR Chemical, Canada). The samples were placed on a roller table (Stuart Roller Mixer, Bibby Scientific, UK) for 16 h, after which the solution was centrifuged at 1500 rpm for 15 min and filtered through a 0.45 μm PES filter (VWR, Canada).

Finally, REE concentrations in both total digested and targeted extractions were analyzed via triple quadrupole inductively coupled plasma mass spectrometry (ICP-MS) (Agilent 8900 ICP-QQQ-MS, Agilent Canada) after filtration on a 0.45 μm PES syringe filter (VWR, Canada) and dilution of 600 μL to 15 mL in 4 % HNO_3 (for total REE) or 2 % trace-metal grade HCl (for leached REE). Iridium (Ir) was used as an internal standard (SCP Chemicals, Canada). Promethium (Pm) was not measured due to its lack of stable isotopes. Since no CRM exists for partial extraction, precision was assessed using measurements ($n = 10$) of an in-house standard, with a coefficient of variation of ±10 %.

2.4. Data treatment and calculation of proxies

We present both REE concentration profiles and REE signatures. The signatures were built as follows. First, REE concentrations were normalized to the North American Shale Composite (NASC) values, which serve as a geological reference representative of the Earth's crust (Rollinson and Pease, 2021) allowing for the identification of REE depletion or enrichment relative to neighboring elements in the periodic table (Gromet et al., 1984). Chondrite values, representing the concentration of REE found in the solar system, and shale average values, representing REE concentration averages at different geographical locations, are two possible bases for comparison (Rollinson and Pease, 2021). Overall, chondrite-normalized signatures are less straightforward compared to shale-normalized ones because the former reflect processes occurring between the formation of the Earth and the formation of sediment, whereas shale-normalization shows processes against the background sediment composition (Rollinson and Pease, 2021). Here, we used the NASC because of its wider usage in the geochemical community (Gromet et al., 1984).

Concentrations were also normalized to Praseodymium (Pr) to reduce the effect of the absolute concentrations when comparing signatures of cores with low and high REE concentrations (Abbott et al., 2015). REE were grouped into light- (LREE) (La to Nd), medium- (MREE) (Samarium (Sm) to Dysprosium (Dy)) and heavy-mass REE (HREE) (Holmium (Ho) to Lu) to allow calculations of three indices: (i) Ce anomaly, (ii) MREE:LREE ratio, and (iii) similarity index.

The Ce anomaly represents the relative enrichment or depletion of Ce compared to its neighboring elements. Since Ce can exist under the Ce (III) or Ce(IV) oxidation states, with Ce(IV) being less soluble than Ce (III) (Rollinson and Pease, 2021), oxidizing conditions are thought to enrich the samples in total Ce. It can be used as a redox condition indicator (Tostevin et al., 2016). The anomaly value is obtained by the equation:

$$Ce_{anomaly} = \frac{Ce_N}{\sqrt{La_N * Pr_N}} \qquad \text{Equation 1}$$

Where Ce_N, La_N and Pr_N represent the normalized concentrations of those elements. A value lower than 0.95 indicates a negative anomaly and a value greater than 1.05 indicates a positive anomaly (Rollinson and Pease, 2021).

The MREE:LREE ratio is a numerical value that serves as a proxy in signature plots (Haley et al., 2004) to enable quantitative comparison. It is calculated here by dividing the average normalized MREE by the average normalized LREE.

The similarity index (SI) uses the MREE:LREE ratio of selected endmembers to determine the relative contributions (with values between 0 and 1) of those endmembers to a station's signature. The SI values were determined as:

$$SI = \frac{\sum |C_{ix} - C_{i1}|}{\sum |C_{ix} - C_{i1}| + \sum |C_{ix} - C_{i2}|} \qquad \text{Equation 2}$$

Where i represents the element or ratio of elements used for determining the specific SI, C_{ix} represents the content of i at the site under consideration, while C_{i1} and C_{i2} represent the content of i at each of the two endmembers (Fei et al., 2017).

3. Results

3.1. REE concentrations and spatial distribution of REE signatures

Measured concentrations of leached La, Ce, Eu and Gadolinium (Gd) are shown in Fig. 3. The profiles are grouped by region, showing that concentrations are an order of magnitude higher in the Beaufort Sea Margin and the Amerasian Basin than on the Bering or Chukchi Shelves. In the Amerasian Basin, concentration profiles show an increase with depth, with Ce peaking between 8 and 14 cm depth in cores S18 and S26. Additionally, La, Ce and Eu all peak at the same depths in core S26. Total and residual REE concentrations vary much less within a region compared to the leached fraction. Furthermore, the leached REE fraction constitutes a significant part of the total REE (Fig. 4). For all MREE, the ratio of leached to total is approximately 0.6 close to the Mackenzie Delta (Stn 380), whereas it drops as low as 0.25 in the Amerasian Basin (Stn S26).

NASC and Pr-normalized concentrations as a function of an element's mass from the Mackenzie Region sites all exhibit a similar signature (Fig. 5). Not only are these signatures homogeneous within the region, but they also show no considerable variation with depth in the sediment cores. Based on these results, an average Mackenzie Signature is provided in Fig. 6 to serve as a basis for comparison.

Signatures from the Bering Sea and Chukchi Sea sites (Fig. 5) show a slight enrichment in MREE, although the magnitude of this enrichment is less than for the Mackenzie Region sites. The Barrow Canyon (Fig. 5) diverges further from the Mackenzie Signature, with a notable relative enrichment of MREE at stations BC-4 and BC-6. A slight signature difference is also seen between the top and bottom of cores in the Barrow Canyon. The signatures from the Beaufort Sea Margin closely resemble those from the Mackenzie Region, but with less pronounced enrichments and depletion, i.e., the MREE area of the signature plot is flatter compared to the Mackenzie Signature. The deepest sites in the Amerasian Basin (S11, S18, S26; Fig. 5) show the greatest differences from signatures from the Mackenzie Region. These sites display a relative enrichment of MREE compared to both lighter and heavier REE, though this enrichment gradually decreases moving northward, with S26 exhibiting the least pronounced enrichment. This region is also where a positive Ce anomaly emerges, reaching an excess of 1.44 in the deep basins. Samples from the M'Clure Strait show enrichment in LREE

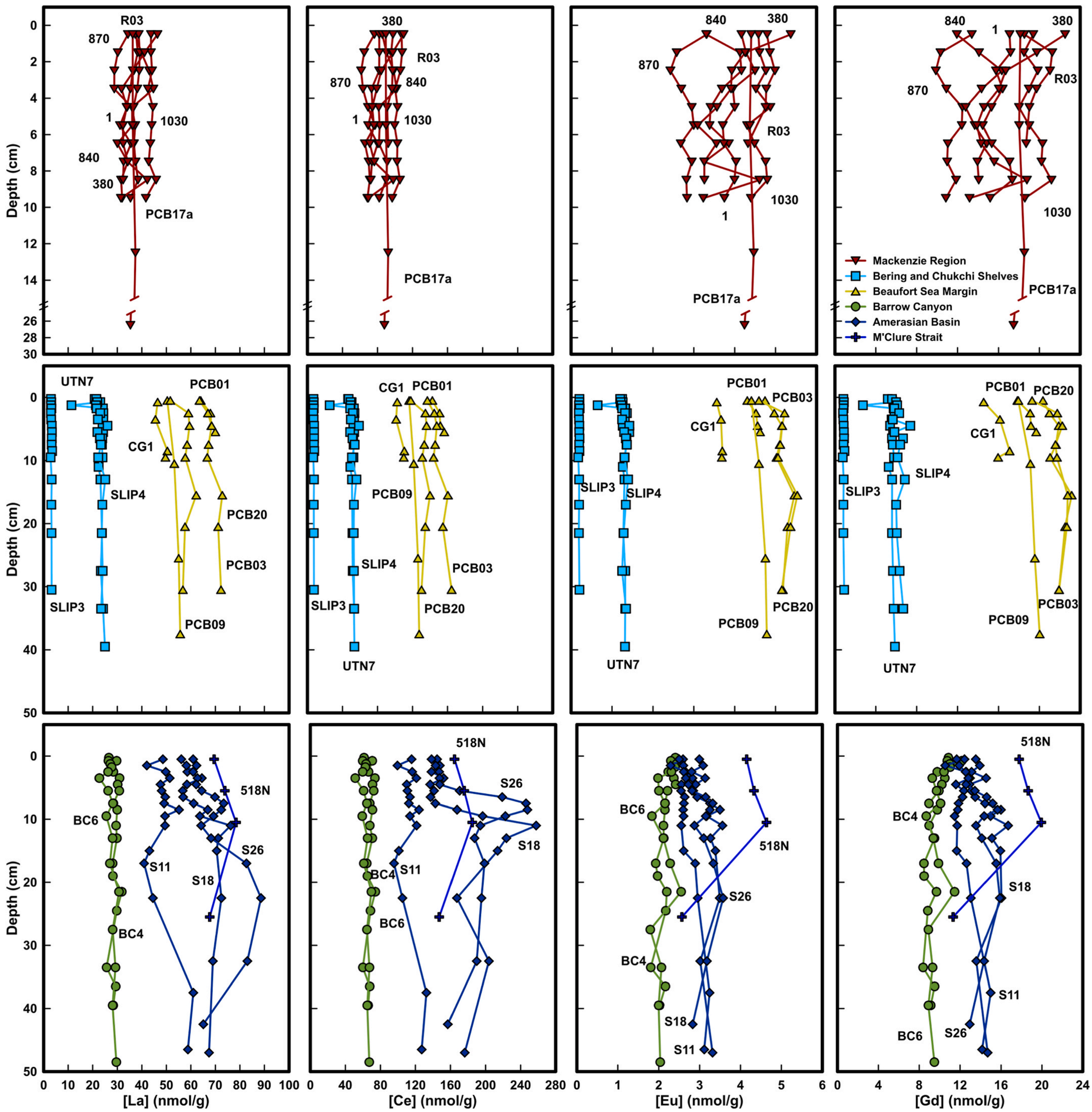

Fig. 3. Concentration profiles of leached La, Ce, Eu and Gd as a function of depth for each site for the Mackenzie Region (inverted triangles on the upper panels), the Bering and Chukchi Shelves (squares on the middle panels), the Beaufort Sea Margin (triangles on the middle panels), Barrow Canyon region (circles on the lower panels), the Amerasian Basin (diamonds on the lower panels) and M'Clure Strait (crosses on the lower panels).

relative to the HREE, while also exhibiting a "medium REE bulge" [(Abbott et al., 2015); (Haley et al., 2004)], similar to the average Mackenzie Signature.

3.2. Depth profiles of normalized REE ratios

MREE:LREE ratio profiles for the Mackenzie Region (Fig. 7) range between 1.7 and 2.3, with little variation with depth. The Bering and Chukchi Shelves exhibit lower MREE:LREE ratios ranging from 1.4 to 1.6, without overlapping with the Mackenzie Region average. In contrast, the Barrow Canyon cores exhibit values between 1.6 and 2.0 that almost reach those of the Mackenzie Region towards the top of the cores. In the Beaufort Sea Margin, MREE:LREE ratio profiles are constant with depth in the core, but the MREE:LREE ratio values are higher at sites closer to the Mackenzie Delta (e.g., PCB09 and PCB20), and approach the Mackenzie Region average. Finally, profiles of the Amerasian Basin sites are distinct from the other regions, showing substantial variation with depth and overall lower MREE:LREE ratios throughout the cores.

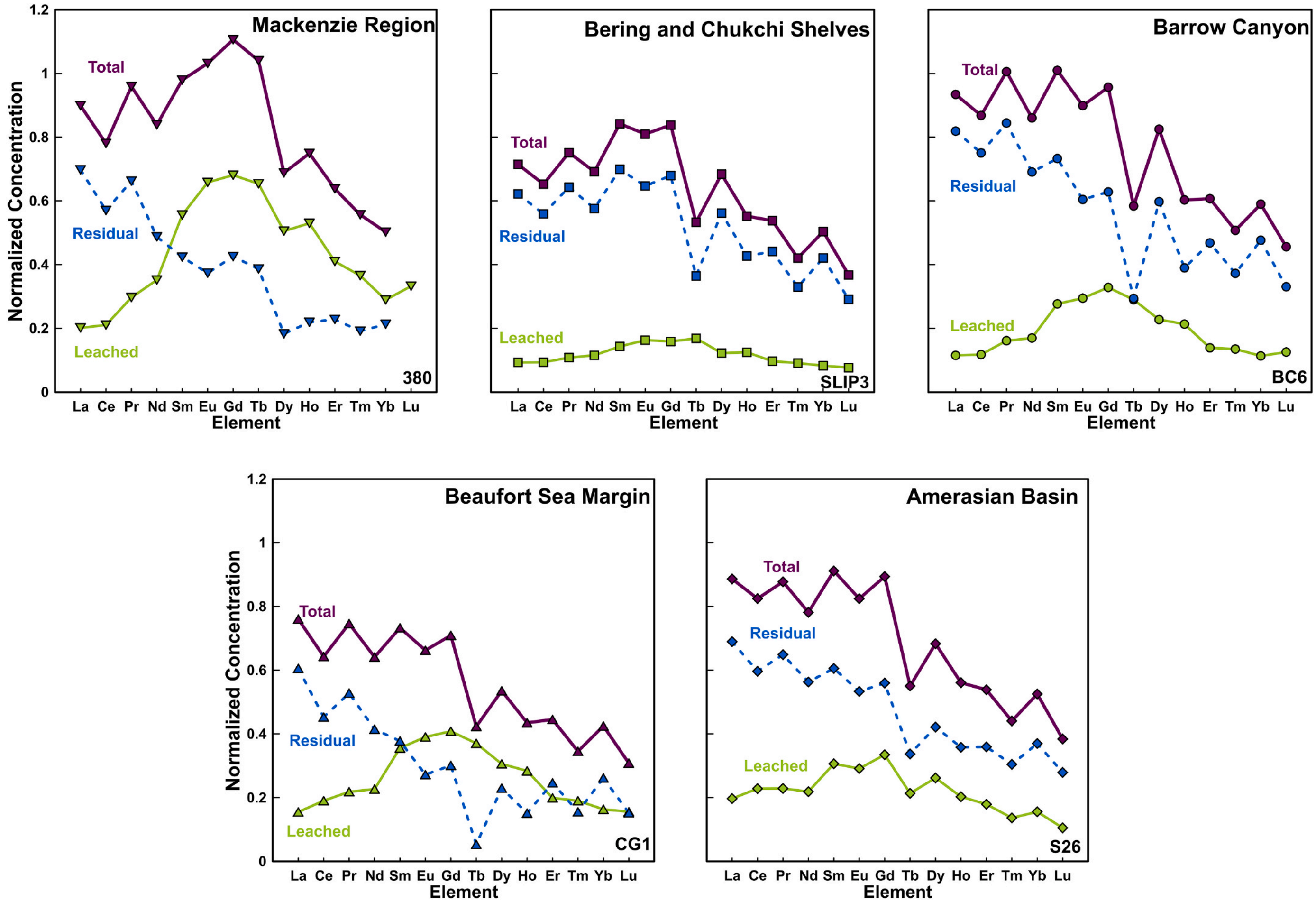

Fig. 4. NASC-normalized REE signatures for the total (purple), leached (green) and calculated residual (total minus leached; blue) fractions from surface sediments of representative sites from the five main study regions, namely stations 380, SLIP3, BC6, CG1 and S26.

4. Discussion

4.1. Factors influencing REE concentration profiles and ratio profiles in the sediments

In this study, we found that the highest proportion of leached REE is present in the Mackenzie Region sediments, and that this proportion diminishes with increasing distance from the delta (Fig. 4). This trend suggests that leached REE changes from source to sink as it travels to the seafloor. Although we cannot definitively ascertain the processes involved, one plausible mechanism is the exchange of particle-reactive substances during particle transport. This process is referred to as "boundary scavenging" [(Kuzyk et al., 2013); (Bacon et al., 1976)], and may enrich particles in labile REE as they exit the Mackenzie Delta into the coastal mixing zone. Leached signatures, as well as the ratio total: leached, are similar among coastal sites, consistent with such scavenging occurring in coastal waters.

Variation of REE signatures with depth in sediment cores has been attributed to changes in sediment sources over time (Fei et al., 2017). The relatively stable signatures over depth and thus over time in most cores suggest that the relative influence of the Mackenzie region on these sites has remained constant. The two exceptions are the Barrow Canyon cores and the Amerasian Basin cores. In the Barrow Canyon sites, a recent shift toward the Mackenzie Signature points to an increasing relative influence of the Mackenzie River over the past two to five decades, consistent with documented increases in the export of suspended particulate matter from the river (Tarasenko et al., 2023).

In the Amerasian Basin, depth profiles of Ce concentrations exhibit more variability compared to other regions (Fig. 8). Our data shows Ce anomalies at sites S18 and S26, which align with previous observations (Ye et al., 2019a). These anomalies likely result from diagenetic processes rather than from direct inputs, as they occur in oxidizing sediments with high oxygen penetration and low organic carbon fluxes at this site (Macdonald and Gobeil, 2011). This has implication for using REE as sediment source tracers, suggesting that REE signatures may not persist over the timescale of millennia [(Liu et al., 2019); (Zhang and Shields, 2022)] characteristic of the Amerasian Basin sediment.

4.2. Spatial persistence of the mackenzie REE signature

We present an average signature for the Mackenzie Region data, referred to as the "Mackenzie Signature" (Fig. 6). The Mackenzie Signature shows a relative enrichment in MREE compared to both heavier and lighter REE, a pattern previously noticed as the MREE bulge. Prior research has shown that the preferential scavenging of MREE is influenced by the mineral composition of the particles, with carbonates, Fe-Mn oxides, apatite and organic matter all linked to MREE enrichment (Lim et al., 2014). Among our normalized measurements, Gd shows the highest values (2.5 ± 0.1; Fig. 6), which falls within the range of natural Gd anomalies (1.20–1.35) and aligns with previously reported natural values of 1.3 (Lafrenière et al., 2023), well below the anthropogenic signal typically ranging from 15 to 100.

Below, we compare other signatures to the Mackenzie Signature and quantify their compositional similarity using similarity index (SI) values. Although our SI values do not represent the mixing of two sediment sources — since the only source for which we have a signature

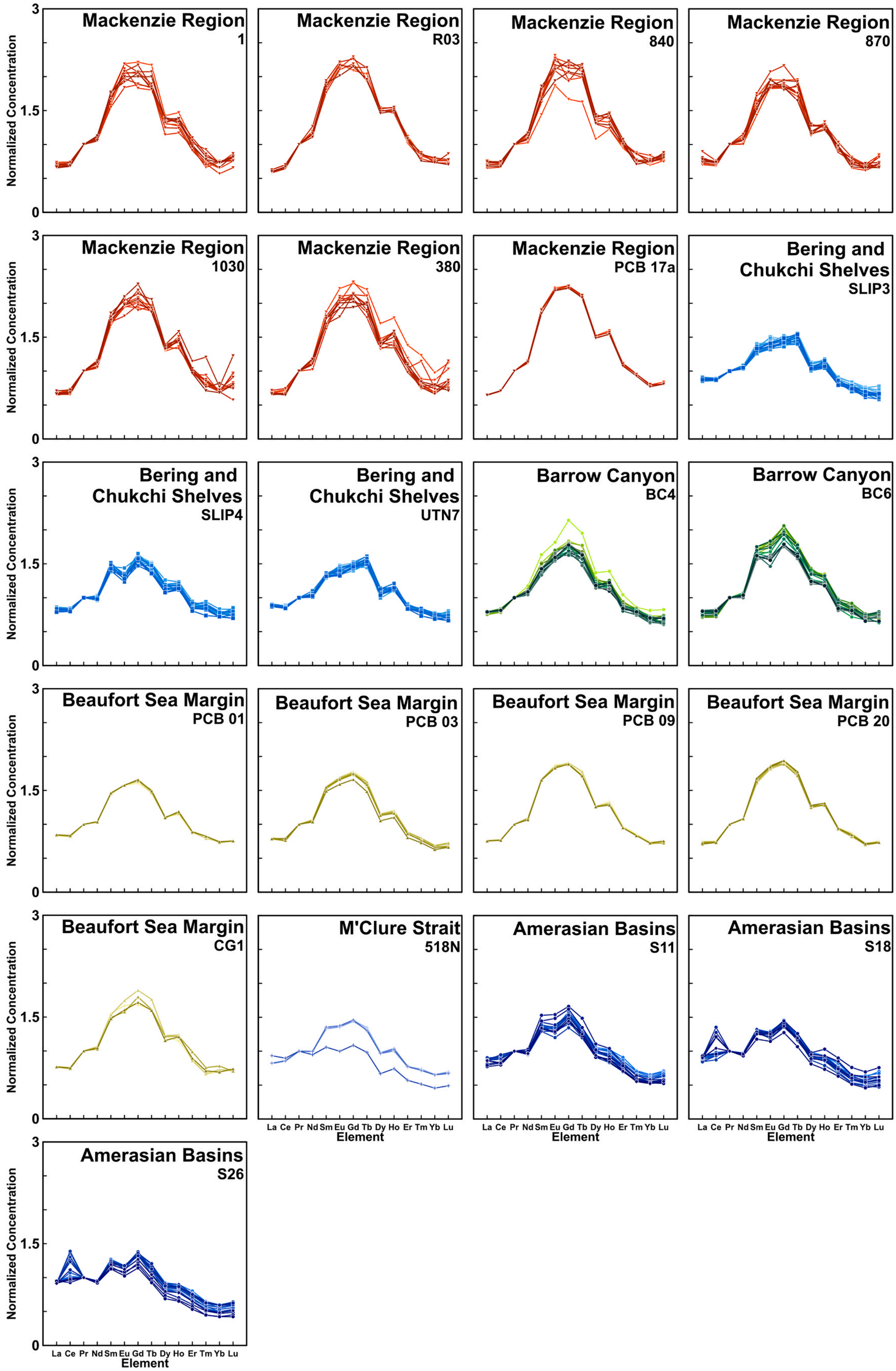

Fig. 5. NASC and Pr-normalized leached REE signatures from the Mackenzie Region, the Bering and Chukchi Shelves, the Beaufort Sea Margin, Barrow Canyon and the Amerasian Basin for each layer of the sediment cores. Lighter lines indicate surface samples.

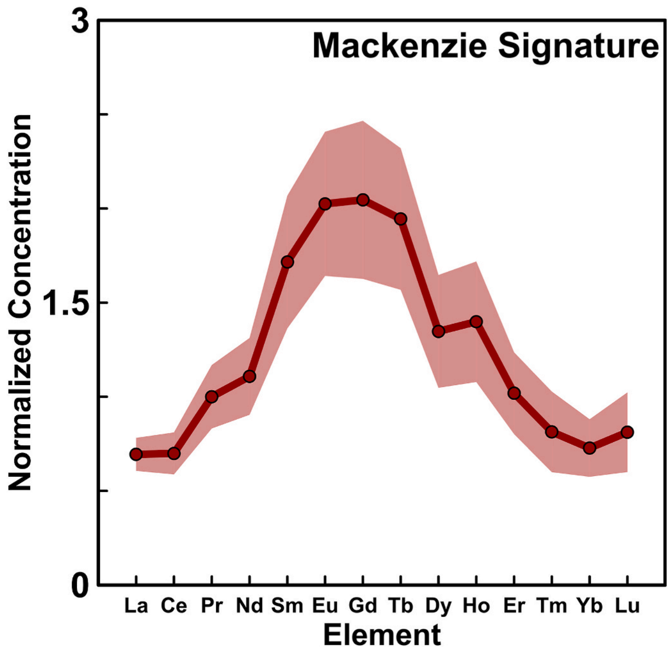

Fig. 6. Average NASC and Pr-Normalized leached signatures (circles) for all the Mackenzie Region samples. The shaded area indicates the standard deviations (n = 57).

is the Mackenzie River — they represent the relative contributions of distinct patterns to the overall signature. We used Station 1, located upriver in the Mackenzie Delta, as the most terrestrial site, and S26, in the Amerasian Basin, as the most distant site. We also used two distinct ratios (MREE:LREE and La:Lu) to compute the signatures. A value closer to 1 represents a strong influence of the Mackenzie River while a value closer to 0 represents a weak influence (color scales on Figs. 1 and 2; numerical values in Table 2). Based on the MREE:LREE ratio, we further calculate the average contribution of the Mackenzie to be 68, 68, 35, 24, and 14 % for the Beaufort Sea Margin, the Barrow Canyon, the Bering and Chukchi Shelves, the M'Clure Strait, and the Amerasian Basin, respectively.

The relationship between MREE:LREE ratio and distance from the Mackenzie River mouth is presented in Fig. 9, showing a clear decrease with distance that points to the diminishing influence of Mackenzie River sediments across the Arctic Ocean. When using the Mackenzie Signature as a basis for comparison, we find that the sediment REE signature at the Bering Sea Shelf sites is distinct from that of the Mackenzie Region, showing a slight enrichment in MREE and a pronounced enrichment for LREE. The Chukchi Sea Shelf site displays a nearly identical signature to the two Bering Sea Shelf signatures. Previous modelling and field studies suggest that the primary source of sediment for the Chukchi Sea is the Bering Strait and Sea, driven by the Transpolar drift from the Pacific Ocean (Charette et al., 2020). Studies of strontium (Sr) and Nd isotopes (Asahara et al., 2012) as well as mineralogy [(Ortiz et al., 2009); (Viscosi-Shirley et al., 2003)] further support this, indicating that most sediment in the Chukchi Sea originates from the Yukon River via the Bering Sea and Siberia and the Aleutian-arc volcanics [(Schwab et al., 2021); (Asahara et al., 2012)]. The small contribution of the Mackenzie River shown in our results aligns with established expectations [(Schwab et al., 2021); (Deschamps et al., 2018); (Deschamps et al., 2017)], with our calculated MREE:LREE ratio suggesting that this contribution amounts to 35 %.

The signatures at the Beaufort Sea Margin remain closely aligned with that of the Mackenzie River, exhibiting varying levels of MREE enrichment that decrease with distance from the delta (Fig. 1; Fig. 5).

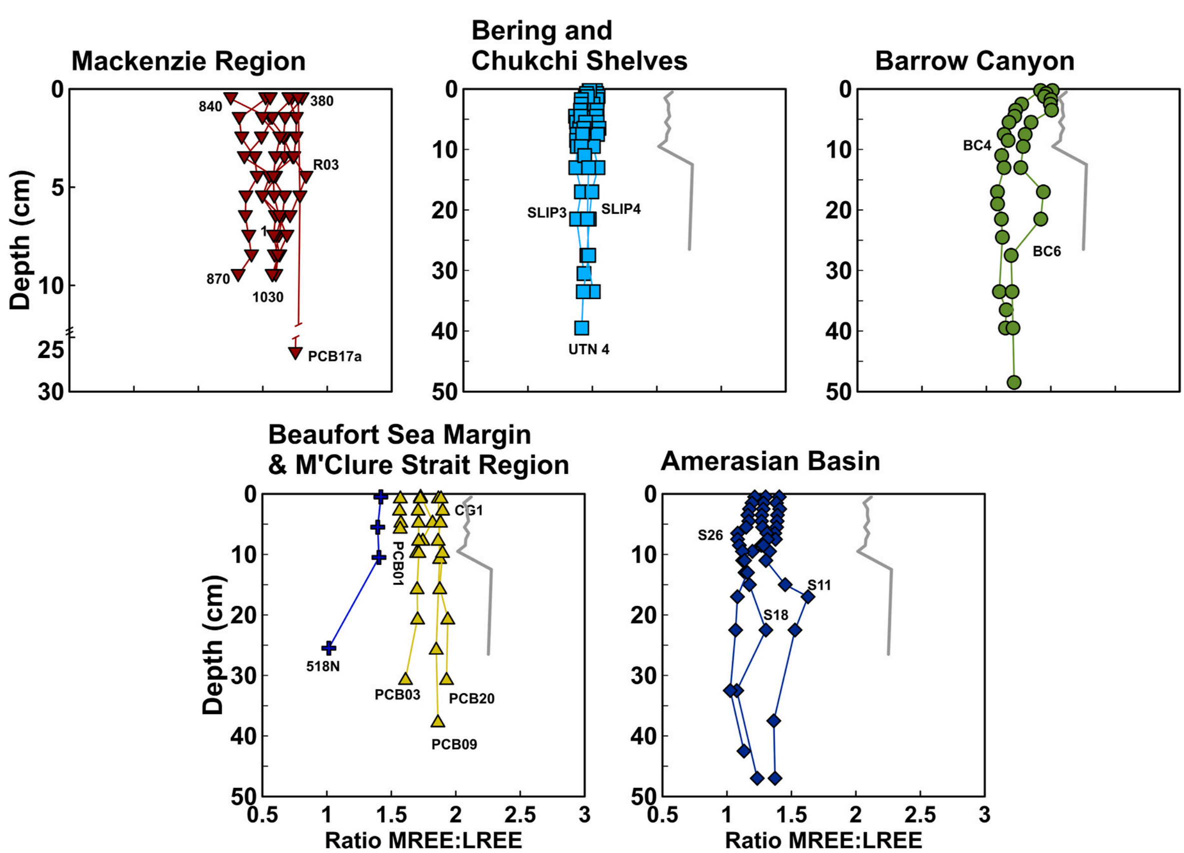

Fig. 7. Leached MREE:LREE ratios (average NASC and Pr-normalized concentrations of MREE over LREE) as a function of depth for the five main regions. Symbols indicate individual cores, and the light grey solid lines represent the average ratios from the Mackenzie.

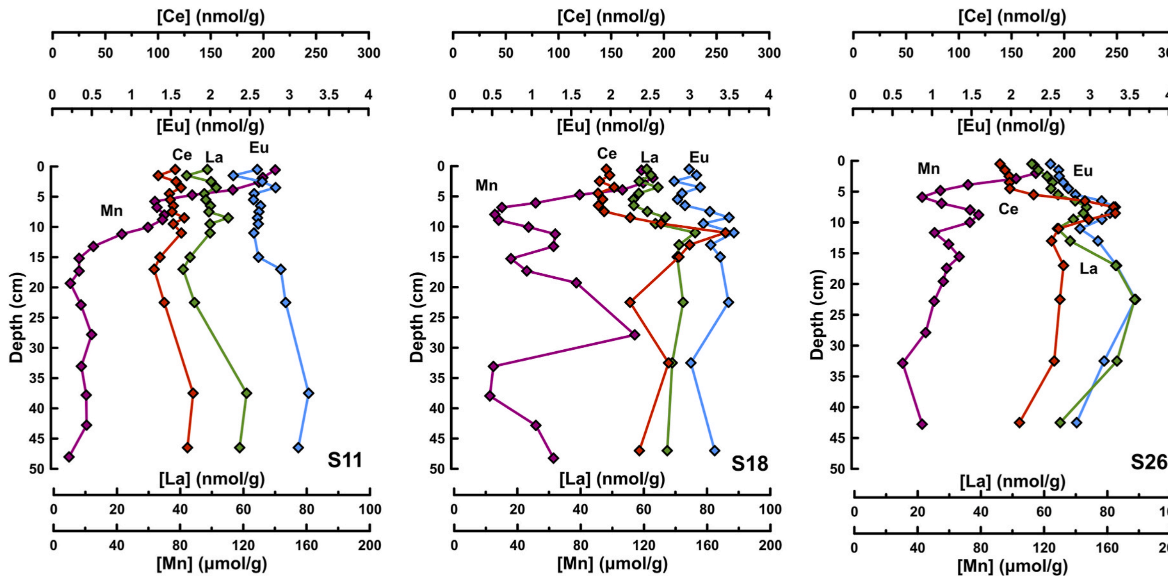

Fig. 8. Concentration profiles of leached Ce (red), La (green), and Eu (blue), as well as total Mn (purple) at three sites in the Amerasian Basin.

Table 2
Similarity indexes (SI) calculated using Stations 1 and S26 as endmembers representative of the Mackenzie Region and the Amerasian Basin, respectively. Two possible ratios to calculate SI are shown. SI values closer to 1 point to higher influence of the Mackenzie Region. MREE = medium-mass REE. LREE = light-mass REE.

Station	MREE:LREE	La: Lu	Geographical Zone
1	1.00	1.00	Mackenzie Region
1030	0.95	0.86	Mackenzie Region
380	0.92	0.88	Mackenzie Region
840	0.91	0.95	Mackenzie Region
R03	0.86	0.91	Mackenzie Region
PCB17a	0.84	0.91	Mackenzie Region
PCB20	0.82	0.86	Beaufort Sea Margin
870	0.82	0.79	Mackenzie Region
BC-6	0.79	0.82	Barrow Canyon
PCB09	0.79	0.82	Beaufort Sea Margin
CG1	0.67	0.77	Beaufort Sea Margin
PCB03	0.61	0.69	Beaufort Sea Margin
BC-4	0.58	0.69	Barrow Canyon
PCB01	0.48	0.72	Beaufort Sea Margin
SLIP-4	0.42	0.77	Bering and Chukchi Shelves
UTN-7	0.34	0.58	Bering and Chukchi Shelves
SLIP-3	0.31	0.43	Bering and Chukchi Shelves
S11	0.29	0.32	Amerasian Basin
518N	0.24	0.46	M'Clure Strait
S18	0.13	0.21	Amerasian Basin
S26	0.00	0.00	Amerasian Basin

This observation is consistent with previous evidence drawn from sedimentary profiles of radio elements ^{137}Cs and ^{210}Pb (Kuzyk et al., 2013). The primary influence on sediments at these sites is expected to come from the Mackenzie River [(Macdonald et al., 1998); (Leitch et al., 2007; Yunker et al., 1993; Macdonald and Thomas, 1991)], given the geographical proximity to the delta's mouth and transport direction of the Beaufort Gyre (Jakobsson et al., 2004). Previous estimates suggest that the Mackenzie River contributes up to 95 % of the total sediments to the region [(Vonk et al., 2015); (Deschamps et al., 2018); (Goñi et al., 2013); (Hill et al., 1991)], with the remaining 5 % contributed by coastal erosion (Vonk et al., 2015).

For Barrow Canyon, our results show that the Mackenzie River is a less important source of sediment (68 %). The northern Barrow Canyon site (BC-6) is more influenced by the Mackenzie River, likely via the Beaufort Gyre [(Klotsko et al., 2019); (Goñi et al., 2013)]. In contrast, the southern site (BC-4) is more influenced by the Chukchi Sea and possibly the Yukon River [(Kuzyk et al., 2017); (Lin et al., 2021); (Pickart et al., 2021); (Klotsko et al., 2019)]. Our calculated SI values at those two sites, from 0.79 in the north to 0.58 in the south, are consistent with this trend, but are higher than previous estimates which showed the Chukchi Sea and Yukon River constituted the majority of sediment imports [(Kuzyk et al., 2017); (McManus et al., 1969)]. In fact, the Barrow Canyon is the only site for which our calculated MREE:LREE ratio appears to overestimate the influence of the Mackenzie River. Determining the MREE:LREE signature of sediments from the Yukon River, a suspected contributor to the Barrow Canyon, would enable better estimates of the contributions of key endmembers.

Westward transport of the Mackenzie River sediment along the Beaufort Sea margin may be attributed to several mechanisms: (1) The Beaufort Gyre, while primarily an anti-cyclonic circulation in deeper waters, has a coastal branch that can transport ice-rafted sediments westward along the Beaufort Shelf edge, especially during periods of strong northeasterly winds (Pickart et al., 2009). (2) Intermittent reversals of the shelf break jet occur during upwelling-favorable wind events, creating easterly flows that can transport suspended sediments westward [(Lin et al., 2019); (Nikolopoulos et al., 2009)]. (3) Sea ice can entrain Mackenzie River sediments during freeze-up in autumn and transport them along irregular trajectories influenced by both the Beaufort Gyre and seasonal wind patterns (Eicken et al., 2005). The combination of these mechanisms likely explains the Mackenzie River signature detected in our Barrow Canyon samples, with the northern site (BC-6) showing stronger Mackenzie influence due to its position closer to the path of the Beaufort Gyre.

Finally, the signature and SI data from the Abyssal Amerasian Basin Region indicate a geochemical dissimilarity to that of the Mackenzie Delta. This finding is consistent with chemical analyses and comparisons of sediment and mineralogical data in the central Arctic Ocean,

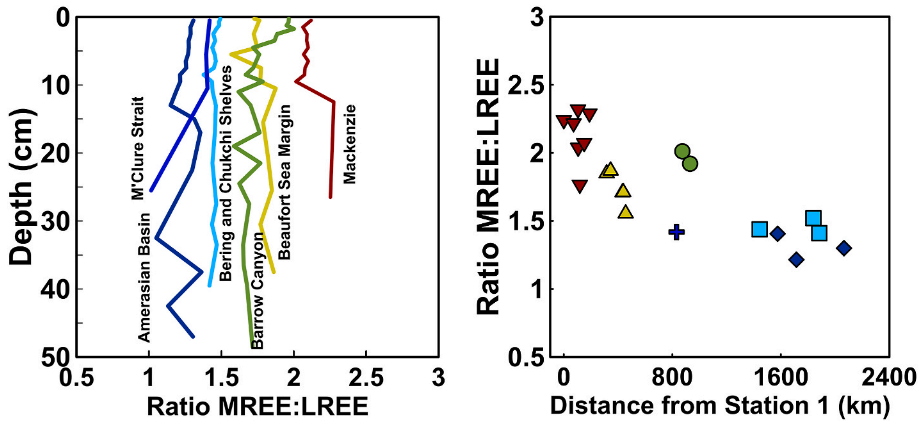

Fig. 9. Average depth profiles of leached MREE:LREE ratios (left panel) and the MREE:LREE ratios as a function of distance from Station 1 (right panel) for the main sampling regions, with symbols corresponding to the regions depicted on Fig. 7.

indicating predominantly Eurasian sources and little contribution from the North American continent [(Martinez et al., 2009); (Kaparulina et al., 2016)]. Nevertheless, the increasing values of the MREE:LREE ratio towards the sediment surface (Fig. 7) could suggest an increasing influence of Mackenzie-type signatures. This potential increase in contributions from the Mackenzie River has been supported by studies utilizing lead (Pb) and neodymium (Nd) isotope measurements in Central Arctic sediments (Fagel et al., 2014). To strengthen this approach, it would be beneficial to identify a distinct Eurasian endmember for REE. In addition, the signatures from M'Clure Strait sediments do not reflect a source from the Mackenzie River, and most likely reflect known sources from the Banks Island and Canadian Archipelago [(Letaïef et al., 2021); (Agnew et al., 2008)]. Most of the sediment reaching this site is transported via drifting sea ice (Letaïef et al., 2021), which is known to contain little sediment derived directly from the Mackenzie River (Darby, 2003).

REE signatures generally result from the sediment sources, the nature of the weathering process prevailing at the site, and the physico-chemical conditions at the onset of sediment genesis [(Lim et al., 2014); (Jung et al., 2021); (Su et al., 2017)]. In this study, an MREE enrichment consistent with metal oxide-humic complexes with REE (Tadayon et al., 2024b) is found in the leached fraction. Although there is no consensus on whether the total or leached REE fractions represent a distinctive signature that remains unchanged during transport and diagenesis [(Jung et al., 2021); (Su et al., 2017); (Tostevin et al., 2016); (Zhang and Shields, 2022)], our calculated proportion of the influence of the Mackenzie River aligns with known sediment sources at our sites. As such, we suggest that leached REE shows a clear influence of the distance from the source.

5. Conclusions

Our data suggest that REE signatures, particularly the MREE:LREE ratio, provide a reliable geochemical fingerprint for tracing sediment sources and transport in the Arctic Ocean. We have established that the contribution from the Mackenzie River decreases with increasing distance from the delta. Our results show that the Mackenzie River supplies up to two-third of the sediments accumulating in the Beaufort Sea Margin and the Barrow Canyon, one-third in the Bering and Chukchi Shelves, and about 15–25% in the M'Clure Strait and deep Amerasian Basin.

Future research should focus on better understanding the processes in the water column that modify the relative distribution of REE. The Beaufort Gyre region, which primarily receives sediment from the Mackenzie River (Jakobsson et al., 2004), represents a valuable natural laboratory to further investigate such REE transport and transformation processes in the Arctic. Future research should also aim to better understand the impact that ongoing climate-driven changes in the carbon cycle will have on REE transport and burial. Finally, it should address the lack of comprehensive REE signature data from other potential sediment sources, particularly from Siberian rivers such as the Lena, the Yenisei and the Ob.

CRediT authorship contribution statement

Thomas Bossé-Demers: Writing – original draft, Methodology, Investigation, Conceptualization. **Charles Gobeil:** Writing – review & editing, Conceptualization. **Bennet Juhls:** Writing – review & editing, Resources. **Martine Lizotte:** Writing – review & editing, Resources, Conceptualization. **Michael Fritz:** Writing – review & editing, Resources, Funding acquisition, Conceptualization. **Lisa Bröder:** Writing – review & editing, Resources, Conceptualization. **Atsushi Matsuoka:** Writing – review & editing, Resources, Conceptualization. **Santiago Mareque:** Writing – review & editing, Investigation. **Raoul-Marie Couture:** Writing – review & editing, Writing – original draft, Validation, Supervision, Project administration, Methodology, Investigation, Funding acquisition, Formal analysis, Conceptualization.

Declaration of competing interest

The authors declare that they have no known competing financial interests or personal relationships that could have appeared to influence the work reported in this paper.

Acknowledgements

We thank the communities of Aklavik, Inuvik and Tuktoyaktuk for their support in the planning and execution of this project. We are thankful to L. Oziel for his devoted help with sampling in the Mackenzie Delta. We acknowledge funding from ArcticNet and the European and Innovation Programme Horizon 2020 for the Nunataryuk (grant no. 773421) and ARICE (grant no. 730965) projects. RMC was funded by the Natural Sciences and Engineering Research Council of Canada (NSERC) through the Discovery Grant program and the Sentinel North program of Université Laval, Canada First Research Excellence Funds. Field logistics was supported, in part, by the Polar Continental Shelf Program (NRC Canada). BJ was funded by the European Space Agency (ESA) as part of the Climate Change Initiative (CCI) fellowship (ESA ESRIN/Contract No. 4000133761/21/I-NB) and the BNP Paribas Foundation with the project “FLO CHAR.” We thank J. Ferland and M.-H. Forget for help with field logistics, S. Groleau and C. Beaulieu for help with instrumental analysis and D. Larivière for allowing and facilitating access to his ICP-MS platform. We thank M. Thaler for editing the manuscript.

Data availability

Data will be made available on request.

References

Abbott, A.N., Haley, B.A., McManus, J., Reimers, C.E., 2015. The sedimentary flux of dissolved rare earth elements to the ocean. Geochem. Cosmochim. Acta 154, 186–200. https://doi.org/10.1016/j.gca.2015.01.010.

Agnew, T., Lambe, A., Long, D., 2008. Estimating sea ice area flux across the Canadian Arctic Archipelago using enhanced AMSR-E. J. Geophys. Res.: Oceans 113 (C10). https://doi.org/10.1029/2007JC004582.

Asahara, Y., Takeuchi, F., Nagashima, K., Harada, N., Yamamoto, K., Oguri, K., Tadai, O., 2012. Provenance of terrigenous detritus of the surface sediments in the Bering and Chukchi Seas as derived from Sr and Nd isotopes: implications for recent climate change in the Arctic regions. Deep-Sea Res Pt Ii 61–64, 155–171. https://doi.org/10.1016/j.dsr2.2011.12.004.

Bacon, M.P., Spencer, D.W., Brewer, P.G., 1976. 210Pb/226Ra and 210Po/210Pb disequilibria in seawater and suspended particulate matter. Earth Planet Sci. Lett. 32 (2), 277–296. https://doi.org/10.1016/0012-821X(76)90068-6.

Bostock, H., Jenkins, C., Mackay, K., Carter, L., Nodder, S., Orpin, A., Pallentin, A., Wysoczanski, R., 2019. Distribution of surficial sediments in the ocean around New Zealand/Aotearoa. Part A: continental slope and deep ocean. N. Z. J. Geol. Geophys. 62 (1), 1–23. https://doi.org/10.1080/00288306.2018.1523198.

Bröder, L., O'Regan, M., Fritz, M., Juhls, B., Priest, T., Lattaud, J., Whalen, D., Matsuoka, A., Pellerin, A., Bossé-Demers, T., Rudbäck, D., Eulenburg, A., Carson, T., Rodriguez-Cuicas, M.-E., Overduin, P., Vonk, J.E., 2022. The Permafrost Carbon in the Beaufort Sea (PeCaBeau) Expedition of the Research Vessel CCGS AMUNDSEN (AMD2104) in 2021. Alfred Wegener Institute for Polar and Marine Research, Bremerhaven.

Carson, M.A., Conly, F.M., Jasper, J.N., 1999. Riverine sediment balance of the Mackenzie delta, northwest territories, Canada. Hydrol. Process. 13 (16), 2499–2518. https://doi.org/10.1002/(sici)1099-1085(199911)13:16<2499::Aid-hyp937>3.0.Co;2-i.

Charette, M.A., Kipp, L.E., Jensen, L.T., Dabrowski, J.S., Whitmore, L.M., Fitzsimmons, J. N., Williford, T., Ulfsbo, A., Jones, E., Bundy, R.M., Vivancos, S.M., Pahnke, K., John, S.G., Xiang, Y., Hatta, M., Petrova, M.V., Heimbürger-Boavida, L., Bauch, D., Newton, R., Pasqualini, A., Agather, A.M., Amon, R.M.W., Anderson, R.F., Andersson, P.S., Benner, R., Bowman, K.L., Edwards, R.L., Gdaniec, S., Gerringa, L.J. A., González, A.G., Granskog, M., Haley, B., Hammerschmidt, C.R., Hansell, D.A., Henderson, P.B., Kadko, D.C., Kaiser, K., Laan, P., Lam, P.J., Lamborg, C.H., Levier, M., Li, X.L., Margolin, A.R., Measures, C., Middag, R., Millero, F.J., Moore, W. S., Paffrath, R., Planquette, H., Rabe, B., Reader, H., Rember, R., Rijkenberg, M.J.A., Roy-Barman, M., van der Loeff, M.R., Saito, M., Schauer, U., Schlosser, P., Sherrell, R.M., Shiller, A.M., Slagter, H., Sonke, J.E., Stedmon, C., Woosley, R.J., Valk, O., van Ooijen, J., Zhang, R.F., 2020. The transpolar drift as a source of riverine and shelf-derived trace elements to the central Arctic Ocean. J Geophys Res-Oceans 125 (5). https://doi.org/10.1029/2019JC015920.

Darby, D.A., 2003. Sources of sediment found in sea ice from the western Arctic Ocean, new insights into processes of entrainment and drift patterns. J Geophys Res-Oceans 108 (C8). https://doi.org/10.1029/2002jc001350.

Darby, D.A., Ortiz, J., Polyak, L., Lund, S., Jakobsson, M., Woodgate, R.A., 2009. The role of currents and sea ice in both slowly deposited central Arctic and rapidly deposited Chukchi-Alaskan margin sediments. Global Planet. Change 68 (1–2), 56–70. https://doi.org/10.1016/j.gloplacha.2009.02.007.

Darby, D.A., Myers, W.B., Jakobsson, M., Rigor, I., 2011. Modern dirty sea ice characteristics and sources: the role of anchor ice. J. Geophys. Res.: Oceans 116 (C9). https://doi.org/10.1029/2010JC006675.

Degen, R., Vedenin, A., Gusky, M., Boetius, A., Brey, T., 2015. Patterns and trends of macrobenthic abundance, biomass and production in the deep Arctic Ocean. Polar Res. 34 (1), 24008. https://doi.org/10.3402/polar.v34.24008.

DeRepentigny, P., Jahn, A., Tremblay, L.B., Newton, R., Pfirman, S., 2020. Increased transnational Sea Ice transport between neighboring arctic states in the 21st century. Earths Future 8 (3), e2019EF001284. https://doi.org/10.1029/2019EF001284.

Deschamps, C.E., St-Onge, G., Montero-Serrano, J.C., Polyak, L., 2017. Chronostratigraphy and spatial distribution of magnetic sediments in the Chukchi and Beaufort seas since the last deglaciation. Boreas 47 (2), 544–564. https://doi.org/10.1111/bor.12296.

Deschamps, C.E., Montero-Serrano, J.C., St-Onge, G., 2018. Sediment provenance changes in the western Arctic Ocean in response to ice rafting, sea level, and oceanic circulation variations since the last deglaciation. Geochem Geophy Geosy 19 (7), 2147–2165. https://doi.org/10.1029/2017gc007411.

Deschamps, C.E., Montero-Serrano, J.C., St-Onge, G., Poirier, A., 2019. Holocene changes in deep water circulation inferred from authigenic Nd and Hf isotopes in sediment records from the chukchi-alaskan and Canadian Beaufort margins. Paleoceanogr. Paleoclimatol. 34 (7), 1038–1056. https://doi.org/10.1029/2018pa003485.

Doxaran, D., Devred, E., Babin, M., 2015. A 50 % increase in the mass of terrestrial particles delivered by the Mackenzie River into the Beaufort Sea (Canadian Arctic Ocean) over the last 10 years. Biogeosciences 12 (11), 3551–3565. https://doi.org/10.5194/bg-12-3551-2015.

Eicken, H., Gradinger, R., Gaylord, A., Mahoney, A., Rigor, I., Melling, H., 2005. Sediment transport by sea ice in the Chukchi and Beaufort Seas: increasing importance due to changing ice conditions? Deep Sea Res. Part II Top. Stud. Oceanogr. 52 (24), 3281–3302. https://doi.org/10.1016/j.dsr2.2005.10.006.

Emmerton, C.A., Lesack, L.F.W., Vincent, W.F., 2008. Nutrient and organic matter patterns across the Mackenzie River, estuary and shelf during the seasonal recession of sea-ice. J. Mar. Syst. 74 (3–4), 741–755. https://doi.org/10.1016/j.jmarsys.2007.10.001.

Fagel, N., Not, C., Gueibe, J., Mattielli, N., Bazhenova, E., 2014. Late Quaternary evolution of sediment provenances in the Central Arctic Ocean: mineral assemblage, trace element composition and Nd and Pb isotope fingerprints of detrital fraction from the Northern Mendeleev Ridge. Quat. Sci. Rev. 92, 140–154. https://doi.org/10.1016/j.quascirev.2013.12.011.

Fei, G., Maosheng, G., Guohua, H., Sen, L., Jing, W., 2017. Source tracing of rare earth elements: a case study of core 07 on the southern coast of Laizhou Bay. Cont. Shelf Res. 136, 29–38. https://doi.org/10.1016/j.csr.2017.01.002.

Fritz, M., Vonk, J.E., Lantuit, H., 2017. Collapsing arctic coastlines. Nat. Clim. Change 7 (1), 6–7. https://doi.org/10.1038/nclimate3188.

Gobeil, C., Macdonald, R.W., Smith, J.N., 1999. Mercury profiles in sediments of the Arctic Ocean basins. Environmental Science & Technology 33 (23), 4194–4198. https://doi.org/10.1021/es990471p.

Goñi, M.A., Yunker, M.B., Macdonald, R.W., Eglinton, T.I., 2000. Distribution and sources of organic biomarkers in arctic sediments from the Mackenzie River and Beaufort Shelf. Mar. Chem. 71 (1–2), 23–51. https://doi.org/10.1016/s0304-4203(00)00037-2.

Goñi, M.A., O'Connor, A.E., Kuzyk, Z.Z., Yunker, M.B., Gobeil, C., Macdonald, R.W., 2013. Distribution and sources of organic matter in surface marine sediments across the North American Arctic margin. J. Geophys. Res.: Oceans 118 (9), 4017–4035. https://doi.org/10.1002/jgrc.20286.

Graf Pannatier, E., 1997. PhD thesis. Sediment accumulation and historical deposition of trace metals and trace organic compounds in the Mackenzie Delta (Northwest Territories, Canada). Faculté des Sciences. Université de Genève, p. 247. https://doi.org/10.13097/archives-ouverte/unige:97977.

Grebmeier, J.M., Cooper, L.W., 1995. Influence of the st. Lawrence island polynya upon the Bering Sea benthos. J. Geophys. Res.: Oceans 100 (C3), 4439–4460. https://doi.org/10.1029/94JC02198.

Gromet, L.P., Dymek, R.F., Haskin, L.A., Korotev, R.L., 1984. The North-American shale composite - its compilation, major and trace-element characteristics. Geochem. Cosmochim. Acta 48 (12), 2469–2482. https://doi.org/10.1016/0016-7037(84)90298-9.

Haley, B.A., Klinkhammer, G.P., McManus, J., 2004. Rare earth elements in pore waters of marine sediments. Geochem. Cosmochim. Acta 68 (6), 1265–1279. https://doi.org/10.1016/j.gca.2003.09.012.

Hill, P.R., Blasco, S.M., Harper, J.R., Fissel, D.B., 1991. Sedimentation on the Canadian Beaufort shelf. Cont. Shelf Res. 11 (8–10), 821–842. https://doi.org/10.1016/0278-4343(91)90081-G.

Hill, P.R., Lewis, C.P., Desmarais, S., Kauppaymuthoo, V., Rais, H., 2001. The Mackenzie Delta: sedimentary processes and facies of a high-latitude, fine-grained delta. Sedimentology 48 (5), 1047–1078. https://doi.org/10.1046/j.1365-3091.2001.00408.x.

Hillaire-Marcel, C., Maccali, J., Not, C., Poirier, A., 2013. Geochemical and isotopic tracers of Arctic sea ice sources and export with special attention to the Younger Dryas interval. Quat. Sci. Rev. 79, 184–190. https://doi.org/10.1016/j.quascirev.2013.05.001.

Holmes, R.M., McClelland, J.W., Peterson, B.J., Shiklomanov, I.A., Shiklomanov, A.I., Zhulidov, A.V., Gordeev, V.V., Bobrovitskaya, N.N., 2002. A circumpolar perspective on fluvial sediment flux to the Arctic Ocean. Glob. Biogeochem. Cycles 16 (4), 45. https://doi.org/10.1029/2001gb001849, 41-45-14.

Holmes, R.M., McClelland, J.W., Peterson, B.J., Tank, S.E., Bulygina, E., Eglinton, T.I., Gordeev, V.V., Gurtovaya, T.Y., Raymond, P.A., Repeta, D.J., Staples, R., Striegl, R. G., Zhulidov, A.V., Zimov, S.A., 2011. Seasonal and annual fluxes of nutrients and organic matter from large rivers to the Arctic Ocean and surrounding seas. Estuaries Coasts 35 (2), 369–382. https://doi.org/10.1007/s12237-011-9386-6.

Ielpi, A., Lapôtre, M.G.A., Finotello, A., Roy-Léveillée, P., 2023. Large sinuous rivers are slowing down in a warming Arctic. Nat. Clim. Change 13 (4), 375–381. https://doi.org/10.1038/s41558-023-01620-9.

Irrgang, A.M., Bendixen, M., Farquharson, L.M., Baranskaya, A.V., Erikson, L.H., Gibbs, A.E., Ogorodov, S.A., Overduin, P.P., Lantuit, H., Grigoriev, M.N., Jones, B. M., 2022. Drivers, dynamics and impacts of changing Arctic coasts. Nat. Rev. Earth Environ. 3 (1), 39–54. https://doi.org/10.1038/s43017-021-00232-1.

Jakobsson, M., Grantz, A., Kristoffersen, Y., Macnab, R., MacDonald, R.W., Sakshaug, E., Stein, R., Jokat, W., 2004. The Arctic Ocean: boundary conditions and background information. In: Stein, R., MacDonald, R.W. (Eds.), The Organic Carbon Cycle in the Arctic Ocean. Springer Berlin Heidelberg, Berlin, Heidelberg, pp. 1–32. https://doi.org/10.1007/978-3-642-18912-8_1.

Juhls, B., Matsuoka, A., Lizotte, M., Bécu, G., Overduin, P.P., El Kassar, J., Devred, E., Doxaran, D., Ferland, J., Forget, M.H., Hilborn, A., Hieronymi, M., Leymarie, E., Maury, J., Oziel, L., Tisserand, L., Anikina, D.O.J., Dillon, M., Babin, M., 2022. Seasonal dynamics of dissolved organic matter in the Mackenzie Delta, Canadian Arctic waters: implications for ocean colour remote sensing. Remote Sensing of Environment 283. https://doi.org/10.1016/j.rse.2022.113327.

Jung, H.-S., Kim, J., Lim, D., Jeong, D., Lee, J., Xu, Z., 2021. REE fractionation and quantification of sediment source in the Yellow Sea mud deposits, East Asian marginal sea. Cont. Shelf Res. 217. https://doi.org/10.1016/j.csr.2021.104374.

Kaparulina, E., Strand, K., Lunkka, J.P., 2016. Provenance analysis of central Arctic Ocean sediments: implications for circum-Arctic ice sheet dynamics and ocean circulation during Late Pleistocene. Quat. Sci. Rev. 147, 210–220. https://doi.org/10.1016/j.quascirev.2015.09.017.

Klotsko, S., Driscoll, N., Keigwin, L., 2019. Multiple meltwater discharge and ice rafting events recorded in the deglacial sediments along the Beaufort Margin, Arctic Ocean. Quat. Sci. Rev. 203, 185–208. https://doi.org/10.1016/j.quascirev.2018.11.014.
Kuzyk, Z.Z.A., Macdonald, R.W., Stern, G.A., Gobeil, C., 2011. Inferences about the modern organic carbon cycle from diagenesis of redox-sensitive elements in Hudson Bay. J. Mar. Syst. 88 (3), 451–462. https://doi.org/10.1016/j.jmarsys.2010.11.001.
Kuzyk, Z.Z.A., Gobeil, C., Macdonald, R.W., 2013. 210Pb and 137Cs in margin sediments of the Arctic Ocean: controls on boundary scavenging. Glob. Biogeochem. Cycles 27 (2), 422–439. https://doi.org/10.1002/gbc.20041.
Kuzyk, Z.Z.A., Gobeil, C., Goñi, M.A., Macdonald, R.W., 2017. Early diagenesis and trace element accumulation in North American Arctic margin sediments. Geochem. Cosmochim. Acta 203, 175–200. https://doi.org/10.1016/j.gca.2016.12.015.
Lafrenière, M.-C., Lapierre, J.-F., Ponton, D.E., Guillemette, F., Amyot, M., 2023. Rare earth elements (REEs) behavior in a large river across a geological and anthropogenic gradient. Geochem. Cosmochim. Acta 353, 129–141. https://doi.org/10.1016/j.gca.2023.05.019.
Lantuit, H., Overduin, P.P., Couture, N., Wetterich, S., Aré, F., Atkinson, D., Brown, J., Cherkashov, G., Drozdov, D., Forbes, D.L., Graves-Gaylord, A., Grigoriev, M., Hubberten, H.-W., Jordan, J., Jorgenson, T., Ødegård, R.S., Ogorodov, S., Pollard, W. H., Rachold, V., Sedenko, S., Solomon, S., Steenhuisen, F., Streletskaya, I., Vasiliev, A., 2012. The arctic coastal dynamics database: a new classification scheme and statistics on arctic permafrost coastlines. Estuaries Coasts 35 (2), 383–400. https://doi.org/10.1007/s12237-010-9362-6.
Larkin, C.S., Piotrowski, A.M., Hindshaw, R.S., Bayon, G., Hilton, R.G., Baronas, J.J., Dellinger, M., Wang, R., Tipper, E.T., 2021. Constraints on the source of reactive phases in sediment from a major Arctic river using neodymium isotopes. Earth Planet Sci. Lett. 565, 116933. https://doi.org/10.1016/j.epsl.2021.116933.
Leitch, D.R., Carrie, J., Lean, D., Macdonald, R.W., Stern, G.A., Wang, F., 2007. The delivery of mercury to the Beaufort Sea of the Arctic Ocean by the Mackenzie River. Sci. Total Environ. 373 (1), 178–195. https://doi.org/10.1016/j.scitotenv.2006.10.041.
Letaïef, S., Montero-Serrano, J.C., St-Onge, G., 2021. Sedimentary processes within the Canadian arctic Archipelago: relationships among sedimentological, geochemical, and magnetic sediment properties. G-cubed 22 (7). https://doi.org/10.1029/2021gc009719.
Lim, D., Jung, H.S., Choi, J.Y., 2014. REE partitioning in riverine sediments around the Yellow Sea and its importance in shelf sediment provenance. Mar. Geol. 357, 12–24. https://doi.org/10.1016/j.margeo.2014.07.002.
Lin, P., Pickart, R.S., McRaven, L.T., Arrigo, K.R., Bahr, F., Lowry, K.E., Stockwell, D.A., Mordy, C.W., 2019. Water mass evolution and circulation of the northeastern Chukchi Sea in summer: implications for nutrient distributions. J. Geophys. Res.: Oceans 124 (7), 4416–4432. https://doi.org/10.1029/2019JC015185.
Lin, P., Pickart, R.S., Våge, K., Li, J., 2021. Fate of warm pacific water in the arctic basin. Geophys. Res. Lett. 48 (20), e2021GL094693. https://doi.org/10.1029/2021GL094693.
Liu, X.-M., Hardisty, D.S., Lyons, T.W., Swart, P.K., 2019. Evaluating the fidelity of the cerium paleoredox tracer during variable carbonate diagenesis on the Great Bahamas Bank. Geochem. Cosmochim. Acta 248, 25–42. https://doi.org/10.1016/j.gca.2018.12.028.
Lizotte, M., Juhls, B., Matsuoka, A., Massicotte, P., Mével, G., Anikina, D.O.J., Antonova, S., Bécu, G., Béguin, M., Bélanger, S., Bossé-Demers, T., Bröder, L., Bruyant, F., Chaillou, G., Comte, J., Couture, R.-M., Devred, E., Deslongchamps, G., Dezutter, T., Dillon, M., Doxaran, D., Flamand, A., Fell, F., Ferland, J., Forget, M.-H., Fritz, M., Gordon, T.J., Guilmette, C., Hilborn, A., Hussherr, R., Irish, C., Joux, F., Kipp, L., Laberge-Carignan, A., Lantuit, H., Leymarie, E., Mannino, A., Maury, J., Overduin, P., Oziel, L., Stedmon, C., Thomas, C., Tisserand, L., Tremblay, J.-É., Vonk, J., Whalen, D., Babin, M., 2023. Nunataryuk field campaigns: understanding the origin and fate of terrestrial organic matter in the coastal waters of the Mackenzie Delta region. Earth Syst. Sci. Data 15 (4), 1617–1653. https://doi.org/10.5194/essd-15-1617-2023.
Macdonald, R.W., Gobeil, C., 2011. Manganese sources and sinks in the Arctic Ocean with reference to periodic enrichments in basin sediments. Aquat. Geochem. 18 (6), 565–591. https://doi.org/10.1007/s10498-011-9149-9.
Macdonald, R.W., Thomas, D.J., 1991. Chemical interactions and sediments of the western Canadian arctic shelf. Cont. Shelf Res. 11 (8), 843–863. https://doi.org/10.1016/0278-4343(91)90082-H.
Macdonald, R.W., Solomon, S.M., Cranston, R.E., Welch, H.E., Yunker, M.B., Gobeil, C., 1998. A sediment and organic carbon budget for the Canadian Beaufort shelf. Mar. Geol. 144 (4), 255–273. https://doi.org/10.1016/S0025-3227(97)00106-0.
Martinez, N.C., Murray, R.W., Dickens, G.R., Kölling, M., 2009. Discrimination of sources of terrigenous sediment deposited in the central Arctic Ocean through the Cenozoic. Paleoceanography 24 (1). https://doi.org/10.1029/2007pa001567.
McManus, D.A., Kelley, J.C., Creager, J.S., 1969. Continental shelf sedimentation in an arctic environment. GSA Bulletin 80 (10), 1961–1984. https://doi.org/10.1130/0016-7606(1969)80[1961:CSSIAA]2.0.CO;2.
Nielsen, D.M., Pieper, P., Barkhordarian, A., Overduin, P., Ilyina, T., Brovkin, V., Baehr, J., Dobrynin, M., 2022. Increase in Arctic coastal erosion and its sensitivity to warming in the twenty-first century. Nat. Clim. Change 12 (3), 263–270. https://doi.org/10.1038/s41558-022-01281-0.
Nikolopoulos, A., Pickart, R.S., Fratantoni, P.S., Shimada, K., Torres, D.J., Jones, E.P., 2009. The western Arctic boundary current at 152°W: structure, variability, and transport. Deep Sea Res. Part II Top. Stud. Oceanogr. 56 (17), 1164–1181. https://doi.org/10.1016/j.dsr2.2008.10.014.
Ortiz, J.D., Polyak, L., Grebmeier, J.M., Darby, D., Eberl, D.D., Naidu, S., Nof, D., 2009. Provenance of Holocene sediment on the Chukchi-Alaskan margin based on combined diffuse spectral reflectance and quantitative X-Ray Diffraction analysis. Global Planet. Change 68 (1–2), 71–84. https://doi.org/10.1016/j.gloplacha.2009.03.020.
Oziel, L., Gürses, Ö., Torres-Valdés, S., Hoppe, C.J.M., Rost, B., Karakuş, O., Danek, C., Koch, B.P., Nissen, C., Koldunov, N., Wang, Q., Völker, C., Iversen, M., Juhls, B., Hauck, J., 2025. Climate change and terrigenous inputs decrease the efficiency of the future Arctic Ocean's biological carbon pump. Nat. Clim. Change. https://doi.org/10.1038/s41558-024-02233-6.
Pickart, R.S., Moore, G.W.K., Torres, D.J., Fratantoni, P.S., Goldsmith, R.A., Yang, J., 2009. Upwelling on the continental slope of the Alaskan Beaufort Sea: storms, ice, and oceanographic response. J. Geophys. Res.: Oceans 114 (C1). https://doi.org/10.1029/2008JC005009.
Pickart, R.S., Spall, M.A., Lin, P., Bahr, F., McRaven, L.T., Arrigo, K.R., Grebmeier, J.M., 2021. Physical controls on the macrofaunal benthic biomass in Barrow Canyon, Chukchi Sea. J. Geophys. Res.: Oceans 126 (5), e2020JC017091. https://doi.org/10.1029/2020JC017091.
Piper, D.Z., 1974. Rare earth elements in the sedimentary cycle: a summary. Chem. Geol. 14 (4), 285–304. https://doi.org/10.1016/0009-2541(74)90066-7.
Rollinson, H., Pease, V., 2021. Using Geochemical Data, 2 ed. Cambridge University Press, Cambridge. https://doi.org/10.1017/9781108777834.
Rood, S.B., Kaluthota, S., Philipsen, L.J., Rood, N.J., Zanewich, K.P., 2017. Increasing discharge from the Mackenzie River system to the Arctic Ocean. Hydrol. Process. 31 (1), 150–160. https://doi.org/10.1002/hyp.10986.
Schwab, M.S., Rickli, J.D., Macdonald, R.W., Harvey, H.R., Haghipour, N., Eglinton, T.I., 2021. Detrital neodymium and (radio)carbon as complementary sedimentary bedfellows? The Western Arctic Ocean as a testbed. Geochem. Cosmochim. Acta 315, 101–126. https://doi.org/10.1016/j.gca.2021.08.019.
Song, Y.H., Choi, M.S., 2009. REE geochemistry of fine-grained sediments from major rivers around the Yellow Sea. Chem. Geol. 266 (3–4), 328–342. https://doi.org/10.1016/j.chemgeo.2009.06.019.
Song, T., Hillaire-Marcel, C., de Vernal, A., Liu, Y., Wang, W., Huang, Y., 2022. A reassessment of Nd-isotopes and clay minerals as tracers of the Holocene Pacific water flux through Bering Strait. Mar. Geol. 443, 106698. https://doi.org/10.1016/j.margeo.2021.106698.
Stadnyk, T.A., Tefs, A., Broesky, M., Déry, S.J., Myers, P.G., Ridenour, N.A., Koenig, K., Vonderbank, L., Gustafsson, D., 2021. Changing freshwater contributions to the Arctic: a 90-year trend analysis (1981–2070). Elementa: Science of the Anthropocene 9 (1), 00098. https://doi.org/10.1525/elementa.2020.00098.
Stein, R., Macdonald, R.W., Naidu, A.S., Yunker, M.B., Gobeil, C., Cooper, L.W., Grebmeier, J.M., Whitledge, T.E., Hameedi, M.J., Petrova, V.I., Batova, G.I., Zinchenko, A.G., Kursheva, A.V., Narkevskiy, E.V., Fahl, K., Vetrov, A., Romankevich, E.A., Birgel, D., Schubert, C., Harvey, H.R., Weiel, D., 2004. Organic carbon in Arctic Ocean sediments: sources, variability, burial, and paleoenvironmental significance. In: Stein, R., MacDonald, R.W. (Eds.), The Organic Carbon Cycle in the Arctic Ocean. Springer Berlin Heidelberg, Berlin, Heidelberg, pp. 169–314. https://doi.org/10.1007/978-3-642-18912-8_7.
Sturgeon, R.E., Desaulniers, J.A.H., Berman, S.S., Russell, D.S., 1982. Determination of trace metals in estuarine sediments by graphite-furnace atomic absorption spectrometry. Anal. Chim. Acta 134, 283–291. https://doi.org/10.1016/S0003-2670(01)84198-2.
Su, N., Yang, S.Y., Guo, Y.L., Yue, W., Wang, X.D., Yin, P., Huang, X.T., 2017. Revisit of rare earth element fractionation during chemical weathering and river sediment transport. Geochem Geophy Geosy 18 (3), 935–955. https://doi.org/10.1002/2016gc006659.
Tadayon, Y., Dutruch, L., Vantelon, D., Gigault, J., Dia, A., Pattier, M., Davranche, M., 2024a. Are nano-colloids controlling rare earth elements mobility or is it the opposite? Insight from A4F-UV-QQQ-ICP-MS. Chemosphere 364, 143164. https://doi.org/10.1016/j.chemosphere.2024.143164.
Tadayon, Y., Vantelon, D., Gigault, J., Dia, A., Pattier, M., Dutruch, L., Davranche, M., 2024b. Rare earth elements interaction with iron-organic matter colloids as a control of the REE environmental dissemination. J. Colloid Interface Sci. 655, 70–79. https://doi.org/10.1016/j.jcis.2023.10.110.
Tarasenko, A., Doxaran, D., Gentili, B., 2023. Variations of suspended particulate matter concentrations of the Mackenzie River plume (Beaufort Sea, Arctic Ocean) over the last two decades. Mar. Pollut. Bull. 196, 115619. https://doi.org/10.1016/j.marpolbul.2023.115619.
Tostevin, R., Shields, G.A., Tarbuck, G.M., He, T.C., Clarkson, M.O., Wood, R.A., 2016. Effective use of cerium anomalies as a redox proxy in carbonate-dominated marine settings. Chem. Geol. 438, 146–162. https://doi.org/10.1016/j.chemgeo.2016.06.027.
Viscosi-Shirley, C., Pisias, N., Mammone, K., 2003. Sediment source strength, transport pathways and accumulation patterns on the Siberian-Arctic's Chukchi and Laptev shelves. Cont. Shelf Res. 23 (11–13), 1201–1225. https://doi.org/10.1016/S0278-4343(03)00090-6.
Vonk, J.E., Giosan, L., Blusztajn, J., Montlucon, D., Pannatier, E.G., McIntyre, C., Wacker, L., Macdonald, R.W., Yunker, M.B., Eglinton, T.I., 2015. Spatial variations in geochemical characteristics of the modern Mackenzie Delta sedimentary system. Geochem. Cosmochim. Acta 171, 100–120. https://doi.org/10.1016/j.gca.2015.08.005.
Xu, Z.K., Lim, D., Choi, J., Yang, S.Y., Jung, H., 2009. Rare earth elements in bottom sediments of major rivers around the Yellow Sea: implications for sediment provenance. Geo Mar. Lett. 29 (5), 291–300. https://doi.org/10.1007/s00367-009-0142-x.
Yang, S.Y., Li, C.X., Lee, C.B., Na, T.K., 2003. REE geochemistry of suspended sediments from the rivers around the Yellow Sea and provenance indicators. Chin. Sci. Bull. 48 (11), 1135–1139. https://doi.org/10.1360/03wd547.

Ye, L.M., März, C., Polyak, L., Yu, X.G., Zhang, W.Y., 2019a. Dynamics of manganese and cerium enrichments in Arctic Ocean sediments: a case study from the alpha ridge. Front. Earth Sci. 6. https://doi.org/10.3389/feart.2018.00236.

Ye, L., März, C., Polyak, L., Yu, X., Zhang, W., 2019b. Dynamics of manganese and cerium enrichments in Arctic Ocean sediments: a case study from the alpha ridge. Front. Earth Sci. 6 (236). https://doi.org/10.3389/feart.2018.00236.

Yunker, M.B., Macdonald, R.W., Cretney, W.J., Fowler, B.R., McLaughlin, F.A., 1993. Alkane, terpene and polycyclic aromatic hydrocarbon geochemistry of the Mackenzie River and Mackenzie shelf: riverine contributions to Beaufort Sea coastal sediment. Geochem. Cosmochim. Acta 57 (13), 3041–3061. https://doi.org/10.1016/0016-7037(93)90292-5.

Zhang, K., Shields, G.A., 2022. Sedimentary Ce anomalies: secular change and implications for paleoenvironmental evolution. Earth Sci. Rev. 229, 104015. https://doi.org/10.1016/j.earscirev.2022.104015.

Zhang, S.M., Mu, C.C., Li, Z.L., Dong, W.W., Wang, X.Y., Streletskaya, I., Grebenets, V., Sokratov, S., Kizyakov, A., Wu, X.D., 2021. Export of nutrients and suspended solids from major Arctic rivers and their response to permafrost degradation. Adv. Clim. Change Res. 12 (4), 466–474. https://doi.org/10.1016/j.accre.2021.06.002.

Zhang, T., Li, D., East, A.E., Walling, D.E., Lane, S., Overeem, I., Beylich, A.A., Koppes, M., Lu, X., 2022. Warming-driven erosion and sediment transport in cold regions. Nat. Rev. Earth Environ. 3 (12), 832–851. https://doi.org/10.1038/s43017-022-00362-0.